

Numerical analysis on stability of express railway tunnel portal

Xiaojun Zhou^{*1}, Hongyun Hu¹, Bo Jiang², Yuefeng Zhou² and Yong Zhu²

¹Key Laboratory of Transportation Tunnel Engineering of China Education Ministry,
School of Civil Engineering, Southwest Jiaotong University, Chengdu 610031, China

²The 1st Design Institute of Civil Engineering and Architecture, China Railway ErYuan Engineering Group
Co. Ltd. Chengdu 610031, China

(Received July 8, 2015, Revised November 17, 2015, Accepted December 1, 2015)

Abstract. On the basis of the geological conditions of high and steep mountainous slope on which an exit portal of an express railway tunnel with a bridge-tunnel combination is to be built, the composite structure of the exit portal with a bridge abutment of the bridge-tunnel combination is presented and the stability of the slope on which the express railway portal is to be built is analyzed using three dimensional (3D) numerical simulation in the paper. Comparison of the practicability for the reinforcement of slope with in-situ bored piles and diaphragm walls are performed so as to enhance the stability of the high and steep slope. The safety factor of the slope due to rockmass excavation both inside the exit portal and beneath the bridge abutment of the bridge-tunnel combination has been also derived using strength reduction technique. The obtained results show that post tunnel portal is a preferred structure to fit high and steep slope, and the surrounding rock around the exit portal of the tunnel on the high and steep mountainous slope remains stable when rockmass is excavated both from the inside of the exit portal and underneath the bridge abutment after the slope is reinforced with both bored piles and diaphragm walls. The stability of the high and steep slope is principally dominated by the shear stress state of the rockmass at the toe of the slope; the procedure of excavating rockmass in the foundation pit of the bridge abutment does not obviously affect the slope stability. In-situ bored piles are more effective in controlling the deformation of the abutment foundation pit in comparison with diaphragm walls and are used as a preferred retaining structure to uphold the stability of slope in respect of the lesser time, easier procedure and lower cost in the construction of the exit portal with bridge-tunnel combination on the high and steep mountainous slope. The results obtained from the numerical analysis in the paper can be used to guide the structural design and construction of express railway tunnel portal with bridge-tunnel combination on high and abrupt mountainous slope under similar situations.

Keywords: tunnel portal; high and abrupt slope; slope stability; safety factor; strength reduction method; numerical simulation

1. Introduction

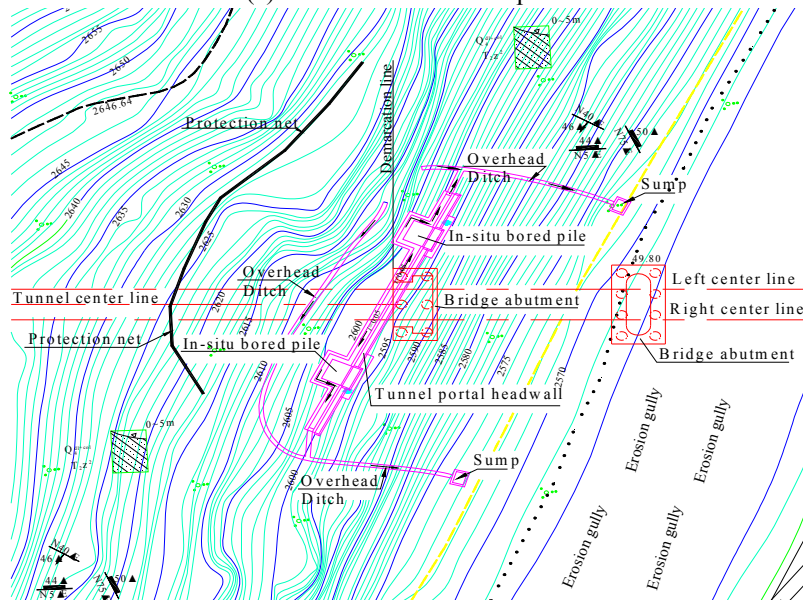
The stability of tunnel portal has been becoming the key crux to be solved when we determine tunnel location in rugged areas. If tunnels are to be built in mountainous regions, this problem may

*Corresponding author, Ph.D., E-mail: zhouxjyu6@sina.com

certainly become more urgent. Whether rockmass around tunnel portal on high and steep mountainous slope is stable or not directly affect the safety of tunnel construction and its long-term service after completion. A series of treatises have been presented to focus on the stability analysis of slopes under different geological conditions and diverse reinforcement methods have been also put into practice. Dawson *et al.* (1999) analyzed the slope stability of a homogenous embankment by means of strength reduction with FLAC code, compared the computed results with that of upper bound limit analysis solution based on a log spiral failure mechanism, they found that the strength reduction results were within a few percent of the limit analysis solutions. Duncan (2000) discussed the simple method to compute factors of safety and reliability in geotechnical engineering practice. Huang Chingchuan *et al.* (2000) proposed a new method for 3D and asymmetric slope stability analysis based upon two-directional moment equilibrium and finally pointed out that the method can be used to calculate the safety factor and possible direction of sliding for semispherical and composite failure surfaces of slopes. Cala *et al.* (2001) investigated the accuracy of shear strength reduction through comparison with conventional limit analysis solutions; their conclusion is that the application of shear strength reduction with FLAC code is proved to be an effective tool in analyzing the stability of complex slope. Zheng *et al.* (2004) discussed the application of strength reduction finite element method (FEM) in analyzing the stability of rock and soil slope, their analysis shows that the average error of safety factor derived from strength reduction FEM is within 5% in comparison with traditional Spencer method. Cheng *et al.* (2007) discussed 3D asymmetrical slope stability analysis with extension of Bishop's, Janbu's, and Morgenstern-Price's Techniques. All of the above-stated scholars focus on the method to analyze slope stability. Other researchers begin to concentrate their focus on the stability of tunnel portal during tunneling. Zhang *et al.* (2008) analyzed the stability and failure surface of a tunnel portal slope using nonlinear FEM and discussed the effectiveness of prestressed anchorage cables applied to keep the stability of tunnel portal slope. Zhang *et al.* (2008) studied the deformation mechanism and stability of a shallow depth tunnel on high slope in a highway using FLAC^{3D}. Li *et al.* (2012) discussed the seismic response of a portal slope and analyzed its stability by means of numerical simulation. Liu *et al.* (2012) made a discussion about the stability of highway tunnel portal in Shiyan area. Unfortunately, few researchers focus upon the stability of express railway tunnel portal with bridge-tunnel combination on high and steep mountainous slope, in addition, technical references relevant to the deformation and safety analysis of express railway tunnel portal and the connection between bridge and tunnel on high and steep slope are not currently available yet. At present, a new express railway line, namely Chengdu-Lanzhou railway, is now under construction in the western China. It starts from Chengdu, the capital of Sichuan Province, and ends at Lanzhou, the capital of Gansu Province, whose total length in the first phase project amounts to 457.59km, of which tunnels and bridges account for 86.06% (Zhou *et al.* 2014). This means a good many of tunnels and bridges are to be built in the railway line because of the rough landform in the mountainous region. In order to analyze the stability of rockmass around entry and exit portal of high speed railway tunnel on high and steep mountainous slope, a tunnel nominated Wang Deng in the railway line is selected to be the object of study in the paper; it is 6605 m long; and its maximum overburden depth reaches 880 m. The ground altitude varies from 2350 m to 3460 m in the region; its relative height difference alters from 400 m to 800 m, in addition, the slope gradient of most mountains generally changes from 30° to 60°, some even reach 80°-90°. So the geomorphology is characterized with high and steep slopes, and most of the lands teem with abrupt precipices and erosion gullies (Zhou *et al.* 2014). The exit portal of Wang Deng tunnel in the new railway line is a typical one. According to site geological investigation, the dip angle of the slope on which Wang Deng tunnel is to be built



(a) Front view of the exit portal



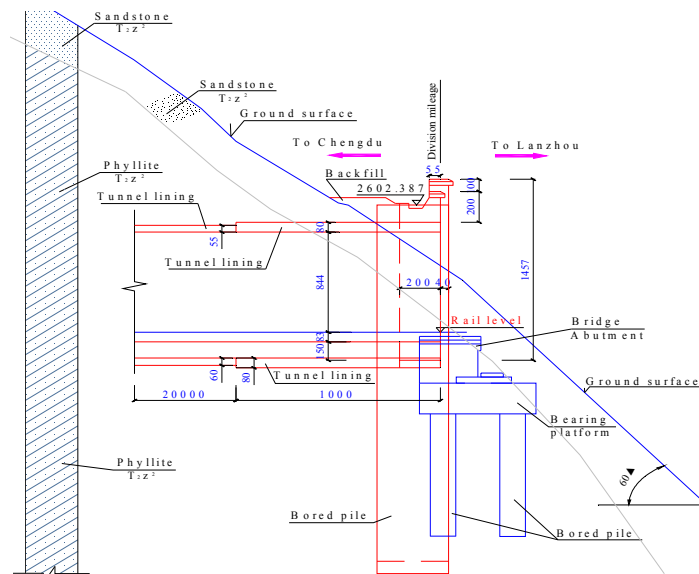
(b) Topographic map of the exit portal

Fig. 1 Landform of the exit portal of Wang Deng tunnel

comes up to 60° , and the altitude varies from 2500 m to 3380 m, so the hypotenuse of the slope where the portal is to be built approximately amounts to 1020 m, therefore the slope is categorized to be a high and steep one. Since the detritus of the completely weathered phyllite in the surface layer of the slope is conducive to cultivating natural flora, so the slopes are covered with thick vegetation. The topographic view and landform of the slope concerned in the paper are shown in Fig. 1 respectively.

2. Structural design of the tunnel portal

According to the engineering geological and hydrogeological conditions of the high and abrupt



(b) Profile of the tunnel portal

Fig. 2 Continued

the tunnel and beneath the bridge abutment is extremely higher (Kocka *et al* 2003, Kocka *et al* 2005). In order to analyze the deformation of surrounding rock in the high and steep slope during the excavation of rockmass inside the tunnel portal, 3D numerical simulation of both the tunneling procedure of the portal and the driving sequence of rockmass in the foundation pit of the bridge-tunnel combination is also conducted.

3. Three dimensional model of the high and steep slope

According to the topography and geology of the slope on which the exit portal of Wang Deng tunnel with bridge-tunnel combination is to be built, a 3D model is set up using Flac^{3D} code and illustrated in detail in Fig. 3.

Fig. 3(a) illustrates the detailed geometric size of the slope model in rectangular coordinate system yo_z , its width in x axis, which is perpendicular to coordinate system yo_z , is 100m in length. Fig. 3(b) shows the 3D element model of the slope in Flac^{3D} code and the spatial coordinate system by which the slope is set up. The displacement restraints applied to the 3D model are as follows, horizontal restraints of zero displacement are applied to the front and rear surface of the element model both in x and y axes, and the vertical zero displacement on its bottom is applied in the inverse direction of z axis. The two top surfaces in positive z axis including the slope itself are all free of constraints.

According to the Chinese code for design of railway tunnel (TB10003-2005), the surrounding rock in the portal exit section is classified into Grade V. Meanwhile, considering the site construction situation, the tunnel is to be built using conventional method, i.e., drill and blast method. Therefore, its support is composed of primary support and secondary lining on the basis of the principle of New Austrian Tunneling Method (Kocka *et al* 2003). Primary support mainly

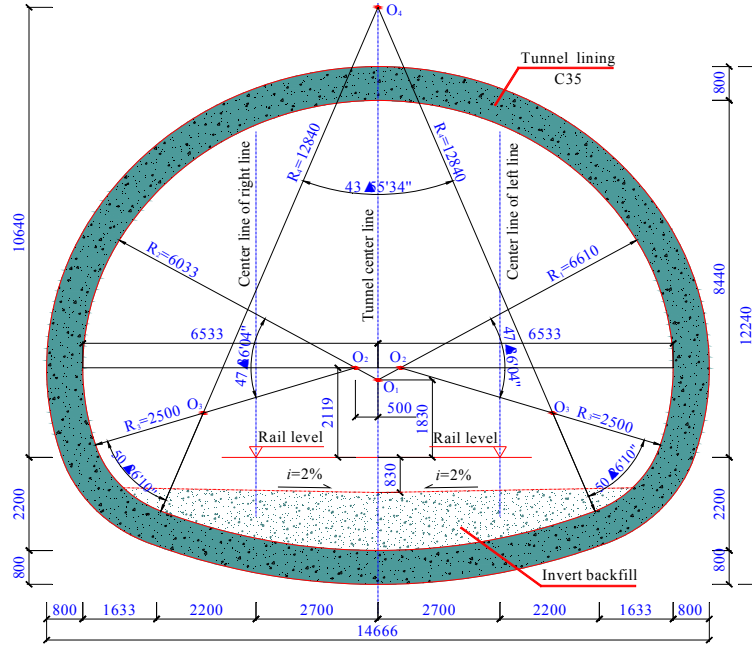


Fig. 5 Cross-section of integral lining for portal exit section (Unit: mm)

layer of phyllite whose surface layer is strongly weathered, this means that phyllite becomes very weak in shear strength, so the portal exit section of tunnel lining is needed to be strengthened so as to sustain rock pressure evoked by loose rockmass and to resist unexpected seismic impact during future service.

Therefore two types of tunnel lining are excogitated to resist surrounding rock in the exit section and as shown in detail in Fig. 2(b) on the basis of empirical design approach and regulations specified in the Chinese design code for railway tunnel. It is clearly seen from Fig. 2(b) that the main difference between the two types of tunnel lining lies in their thickness and length. One type is that the thickness of tunnel lining is designed to be 550 mm and 20 m long in longitudinal length, the other is 800 mm in thickness and 10 m in length in the section outward Wang Deng tunnel portal as shown in Fig. 2(b). The typical details of the two types of tunnel lining for resisting surrounding rock in the portal exit section of Wang Deng tunnel are illustrated in Fig. 4 and Fig. 5 respectively.

According to the basic procedure of casting reinforced concrete support of the tunnel in drill and blast method, primary support is used to resist all rock pressure during tunneling, but secondary lining is employed as a safety reserve for long-term service after the completion of the tunnel. Consequently, in the three dimensional numerical model, only the primary support is taken into account in order to facilitate the numerical simulation. Since steel arch is used as a dominant strut in primary support to restrain excessive rock deformation, its stiffness is converted into the one of the primary support on the basis of the principle of stiffness equivalence. The stiffness of primary support including the stiffness of steel arch support is derived from

$$E = E_{sh} + E_{ar} \frac{A_{ar}}{A_{sh}} \quad (1)$$

Where E is the elastic modulus of primary support, in MPa; E_{sh} denotes the elastic modulus of shotcrete, in MPa; E_{ar} stands for the elastic modulus of steel arch in MPa; A_{ar} refers to the cross-sectional area of steel arch in m^2 , A_{sh} connotes the cross-sectional area of shotcrete support in m^2 .

According to the obtained geological conditions and the code for design of railway tunnel (TB10003-2005), the physico-mechanical parameters of the materials in the 3D numerical model are listed in Table 1.

Table 1 Physico-mechanical parameters of numerical model

Materials	Elastic modulus E (GPa)	Poisson's ratio μ	Unit weight γ (kN/m ³)	Cohesion C (kPa)	Internal friction angle φ (°)
Sandstone	0.50	0.40	21.0	90	17.0
Phyllite	4.70	0.35	27.5	560	35.0
Primary support	21.0	0.22	22.0	/	/
Bored pile	30.0	0.20	25.0	/	/
Diaphragm wall	30.0	0.20	25.0	/	/

It has been practically proved that the role of systematic rockbolt installed in the surrounding rock of tunnels is to reinforce jointed rockmass, restrain excessive rock deformation and maintain rock stability (Zhu *et al* 2003, Carranza-Torres 2009).

In order to simplify the numerical simulation, the reinforcement of systematic rockbolt in surrounding rock around the tunnel is taken into account in the numerical modeling by enhancing the shear strength parameters of the surrounding rock within the predesigned range of reinforcement.

Furthermore, in order to analyze the stability of the slope due to the deformation of surrounding rock subject to tunnel excavation, the strength reduction technique is used and the safety factor F_s to determine the slope stability is derived from following formulae (Dawson *et al.* 1999, Duncan 2000, Cala *et al.* 2001, Zheng *et al.* 2004).

$$C' = \frac{1}{F_s} C. \quad (2)$$

$$\varphi' = \arctan\left(\frac{1}{F_s} \tan \varphi\right). \quad (3)$$

Where C' denotes the reduced value of cohesion of rockmass, in kPa, φ' stands for the reduced value of internal friction angle of rockmass, in °.

If the shear strength of surrounding rock is repeatedly decreased to the limit equilibrium state of the slope according to Eq. (2) and Eq. (3) in the numerical simulation, then F_s is regarded to be its safety factor, and the common values of factors of safety may range from 1.2 to 3.0 (Lee *et al.* 1983). According to the regulation in Chinese code for building slope works (GB50330-2013), tunnel slope belongs to an important slope work affected by itself providing that tunnel is to be built within its influential range, its safety grade is defined as grade one, and the safety factor must be greater than 1.3, that is $F_s \geq 1.3$ when determining the safety of slope works.

The numerical simulation is mainly divided into two steps, one is to simulate the procedure of

Table 2 Mechanical parameters of pile element

Cross-sectional area/(m ²)	Shear cohesive stiffness K_s /(GN·m ⁻²)	Shear cohesive force F_{ss} /(GN·m ⁻¹)	Cohesive shear angle φ_s (°)	Normal cohesive stiffness K_n /(GN·m ⁻²)	Normal cohesive force F_n /(GN·m ⁻¹)	Normal cohesive shear angle φ_n (°)
3.5×3.0	13	0	30	130	100	30

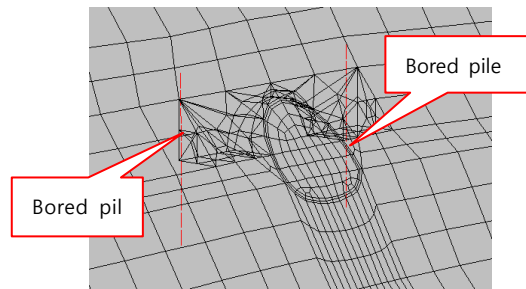


Fig. 6 Bored piles in 3D model

tunneling rockmass inside the contour of the tunnel exit portal, and the other is to simulate the procedure of driving rockmass in the bridge abutment foundation pit just underneath the floor of the exit portal of Wang Deng tunnel.

4. Slope stability due to tunneling in the exit portal

Two cases are simulated in order to determine the stability of the high and steep mountainous slope. One is to simulate the natural state of the slope to which no reinforcement measures are applied, the other is to simulate the state of the slope which is reinforced with bored piles.

Accordingly, on each flank of the exit portal an in-situ bored pile is set up in the rockmass, as a result, two bored piles are erected in the surrounding rock so as to maintain the stability of the high and abrupt slope. The pile element in Flac^{3D} code is used to simulate the anti-slide pile in the numerical model and as shown in Fig. 6, its geometric parameters are determined according to the details in Fig. 2, and its mechanical parameters are tabulated in Table 2.

In addition, the Mohr-Coulomb yield criterion in the Flac^{3D} is employed in the numerical simulation.

In order to analyze the slope stability using shear strength reduction technique, numerical simulations are performed for a series of trial safety factors starting from a value of 0.8. Through numerical simulation of the state of the slope under the above-stated two cases, the shear strain increment in rockmass in the slope is obtained and shown in Fig. 7 and Fig. 8 respectively.

It is seen from Fig. 7 and Fig. 8 that, as the toe of the slope is reinforced with anti-slide piles, the maximum shear strain increment in rockmass in the toe decreases largely from 3.00×10^{-2} to 7.09×10^{-3} .

This indicates that anti-slide piles are effective in controlling the deformation of rockmass in the high and steep slope. The obtained safety factor F_s also increases from 1.21 to 1.75 after the slope is reinforced with bored piles, that is $F_s=1.75 > 1.3$. This is to say that if the slope is not reinforced with

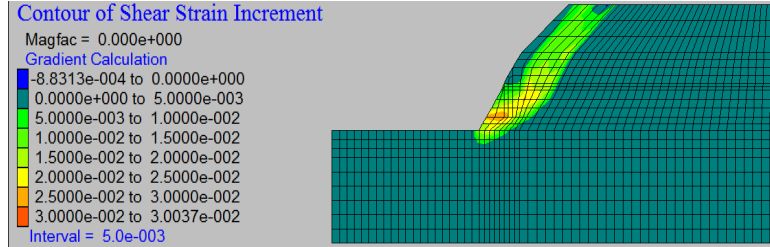


Fig. 7 Shear strain increment in slope without piles

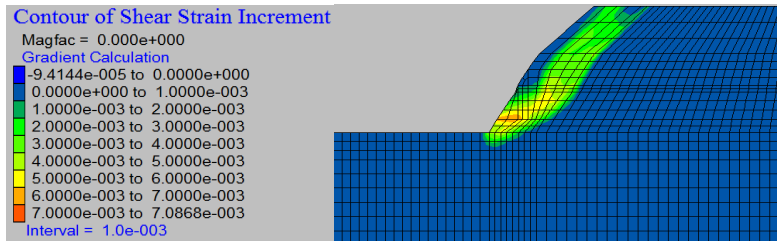


Fig. 8 Shear strain increment in slope reinforced with piles

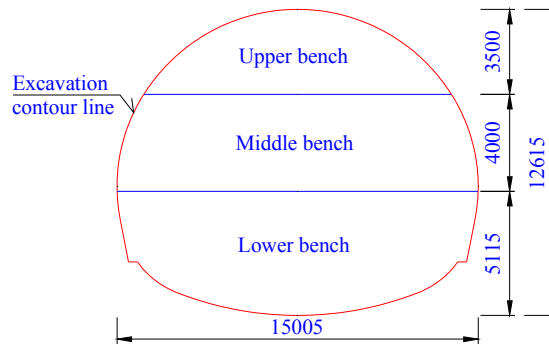


Fig. 9 Driving sequence of rockmass in tunnel portal (Unit: mm)

bored piles, its safety factor only meets $F_s=1.21<1.3$, so the slope is not stable. After it is reinforced with in-situ bored piles, its safety is enhanced. Consequently, it is apparent that anti-slide piles must be set in the rockmass so as to retain the stability of the slope. Since Wang Deng tunnel as well as its exit portal is to be built on the same slope, the next most important step is to analyze the stability of the slope during the procedure of excavating rockmass from the contour inside of the exit portal of Wang Deng tunnel using partial excavation method. According to the driving sequence of the tunneling method, the entire working face of the tunnel portal is mainly divided into 3 benches, namely the upper bench, the middle and the lower one. So the numerical simulation of the tunneling procedure in the portal exit section is still performed so as to determine whether the slope is stable or not during tunneling. The steps to sequentially excavate the rockmass from the outline inside of the exit portal are delineated in Fig. 9.

The tunneling footage of every bench is specified in the driving direction for a fixed distance from another one so as to minimize mutual interference of tunneling during construction in the tunnel. As a result, driving depth for every bench in the numerical simulation is controlled within

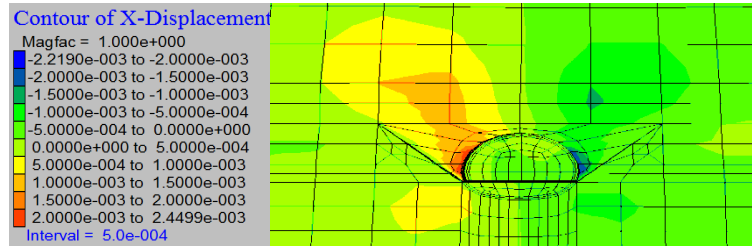


Fig. 10 Isogram of surrounding rock deformation in x axis (Unit: m)

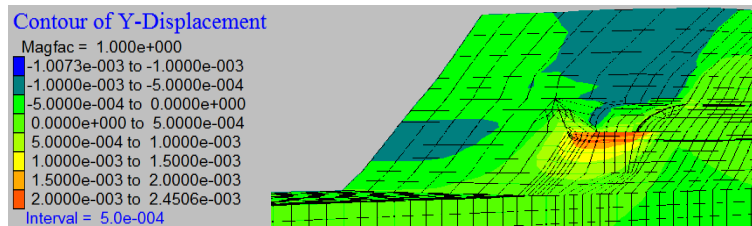


Fig. 11 Isogram of surrounding rock deformation in y axis (Unit: m)

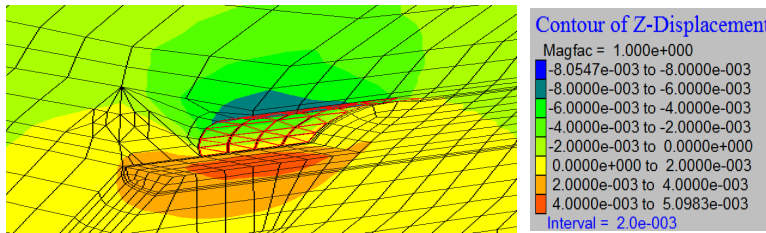


Fig. 12 Isogram of surrounding rock deformation in z axis (Unit: m)

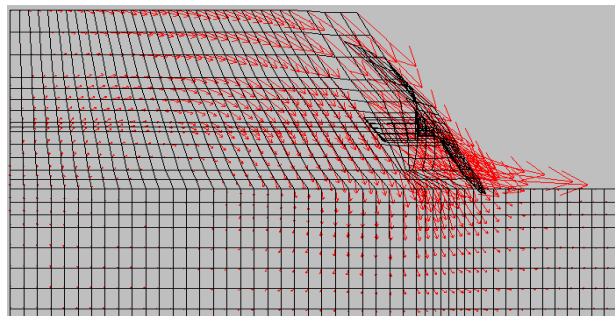


Fig. 13 Displacement vector in slope

1.0 m. The total footage of tunneling in the numerical simulation amounts to 35 m. The isograms of rockmass displacement obtained from numerical simulation in x , y , z axis are shown in Fig. 10, Fig. 11 and Fig. 12 respectively.

It is seen from Fig. 10, Fig. 11 and Fig. 12 that the maximum crown subsidence of the portal supported by primary support reaches 8.1 mm during the tunneling; and the floor upheaval ascends to 5.1 mm. The displacement in positive y axis only reaches 2.5 mm, meanwhile, the horizontal displacement convergence between two sidewalls approximately approaches 4.4 mm. Therefore,

the maximum value of crown settlement due to tunnel excavation does not exceed 10 mm. In order to show the magnitude of displacement occurs in the slope, displacement vector to indicate the trend of rockmass movement due to tunnel excavation in the slope is illustrated in Fig. 13.

Fig. 13 illustrates the displacement vector on each node in the 3D element model; the short red arrows denote the magnitude and direction of rock displacement in the slope due to tunneling. It is apparent that the nodal displacement approaches to the maximum value at the toe of the slope. So the rockmass at this location becomes very weak in strength and possibly collapse during the course of tunneling the exit portal. In order to make an insight into rock deformation on the slope due to excavation of rockmass in the exit portal, some particular points are placed on the front slope in the numerical model so as to observe their displacement during tunneling; their location on the front slope above the exit portal is clearly shown in Fig. 14.

It is easily deduced from Fig. 14 that the displacement at each monitoring point typically reflects the ground subsidence due to tunneling. The relationship between driving depth and ground settlement obtained from numerical simulation is shown in Fig. 15.

It is derived from Fig. 15(a) that the maximum subsidence occurs at point 1 which stands nearest toward the portal, its ultimate value approaches 6.0 mm which is less than that of crown subsidence due to tunneling. Thus, the further the monitoring point is placed from the portal, the less the subsidence it occurs. So it is also elicited from Fig. 15(b) that the maximum subsidence takes place

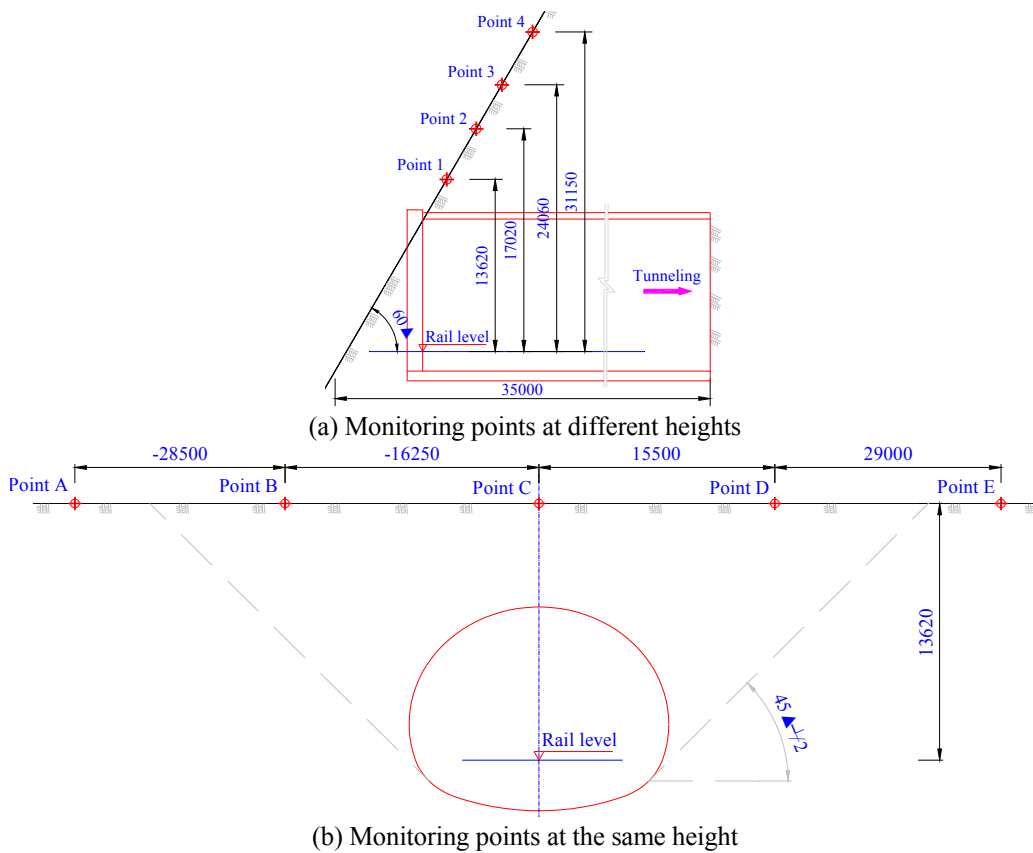


Fig. 14 Displacement vector in slope

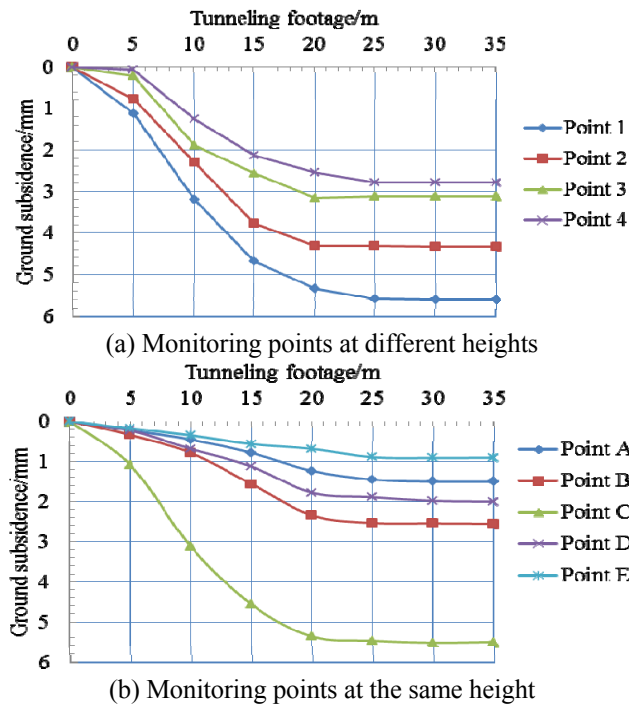


Fig. 15 Relationship between ground subsidence and tunneling footage

at point C which is just above the crown of the tunnel portal, the subsidence occurs at the other four points is much less than that at point C. As a result, tunneling the exit portal of Wang Deng tunnel may lead to the deformation of rockmass on its front slope, whereas the magnitude of deformation does not exceed 10 mm. In order to maintain the stability of surrounding rock at tunnel portal, anti-slide piles must be set up in the endwall of the portal on the slope in the light of the numerical analysis results. The safety factor of the slope stability rises up to 1.75 after the bored piles are erected in the surrounding rock. This also corroborates that the high and steep slope remains stable during the course of driving the exit portal of Wang Deng tunnel providing that it is reinforced with bored piles prior to excavation.

5. Slope stability due to excavating the foundation pit

According to the requirement of connection between bridge and tunnel at the exit portal of Wang Deng tunnel, a bridge abutment must be set up in the floor of the exit portal. Accordingly, a foundation pit is to be excavated in the floor as well. The excavation of foundation pit for the bridge abutment cannot avoid the second impact of rock deformation on the stability of the high and steep slope. In order to dissect the second influence of excavation of foundation pit on the slope stability, the construction procedure of foundation pit has been also simulated using 3D numerical analysis. According to the detailed design of the foundation pit, it is of 6 m wide in y axis, of 12 m wide in x axis and 12 m long in z axis. The numerical model of the foundation pit for bridge abutment in the floor is set up and depicted in Fig. 16.

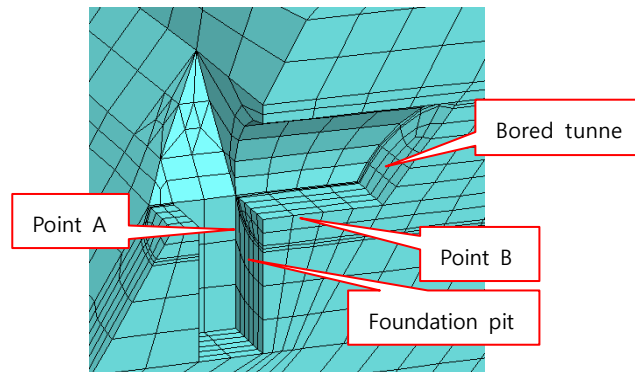


Fig. 16 Displacement vector in slope

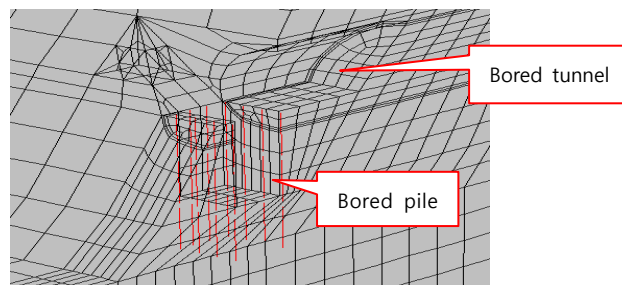


Fig. 17 3D model of bored piles

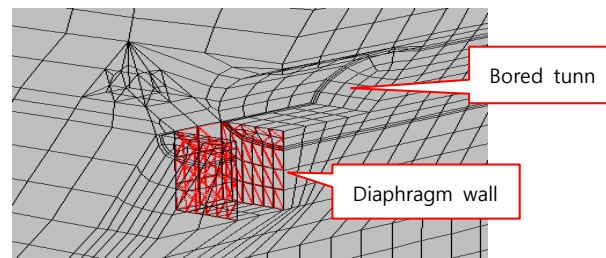


Fig. 18 3D model of diaphragm wall

Since the depth of foundation pit approaches 12 m, so it is necessary to analyze the safety of foundation pit itself. In order to sustain the stability of foundation pit during rock excavation, two retaining structures are set up in the foundation pit. One is in-situ bored piles, the other is diaphragm walls. The bored pile is 0.8 m in diameter and as well as 16 m in length; the diaphragm wall is 0.5 m in thickness, and as well as 16m in depth. Their numerical model in Flac^{3D} code is illustrated in Fig. 17 and Fig. 18 respectively.

The rock deformation due to excavation of rockmass in the abutment foundation pit, which is separately sustained by bored piles and diaphragm walls, are shown in Fig. 19 and Fig. 20 respectively.

It is obtained from Fig. 19 and Fig. 20 that the excavation does not result in larger deformation in the surrounding rock. The isogram of displacement in rockmass around the foundation pit appears to be the same, whereas there is very little difference in the magnitude of rock deformation

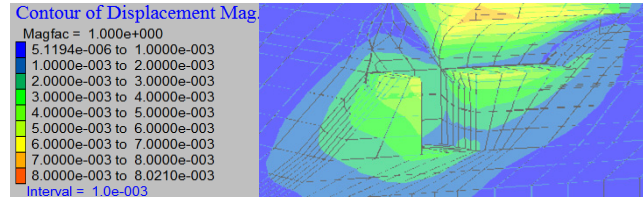


Fig. 19 Displacement of rockmass around foundation pit sustained by bored piles (Unit: m)

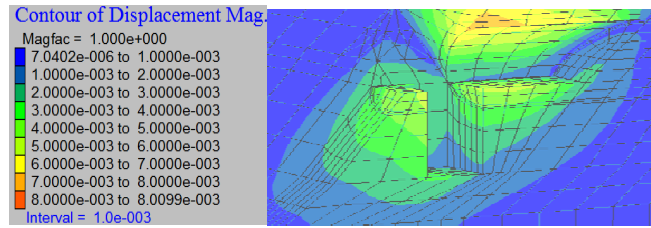


Fig. 20 Displacement of rockmass around foundation pit sustained by diaphragm walls (Unit: m)

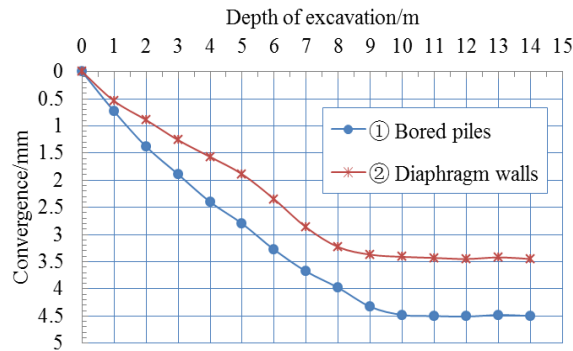


Fig. 21 Relationship between convergence of line AB and excavation depth in the foundation pit

due to the excavation of the foundation pit. It is also seen that the maximum ultimate value of the tunnel crown settlement approaches 8.02 mm.

Additionally, the deformation of rockmass around foundation pit may also affect the stability of the portal exit section. In order to analyze the deformation characteristics of rockmass around the foundation pit during the course of excavating rockmass inside the foundation pit itself, two points A and B are intentionally placed on the top brink of the foundation pit and as shown in Fig. 16. Providing that point A is linked to point B with a straight line, then the variation in length of line AB is obtained when rockmass is excavated in the foundation pit. The length variation of straight line AB definitely shows the deformation features of rockmass around the foundation pit. The relationship between the variation in length of line AB and the excavation depth in the foundation pit is also shown in Fig. 21.

The curve numbered with ① in Fig. 21 is obtained from the simulation of excavating rockmass in the foundation pit supported by bored piles, additionally, the curve numbered with ② is also obtained from the simulation of driving the rockmass in the foundation pit supported by diaphragm walls. It is seen from Fig. 21 that rock deformation due to excavation of rockmass in the foundation pit supported by bored piles converges to 4.5 mm after the completion of rockmass excavation. If

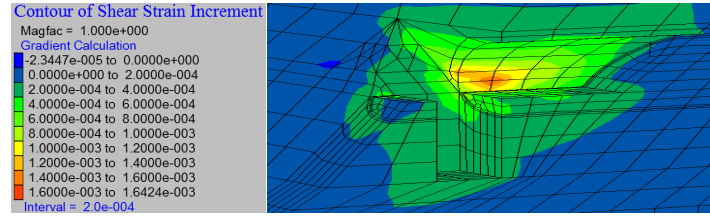


Fig. 22 Shear strain in rockmass around foundation pit sustained by piles (Unit: m)

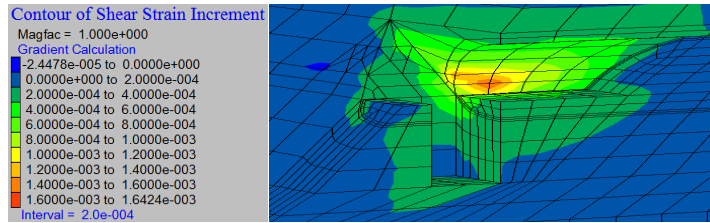


Fig. 23 Shear strain in rockmass around foundation pit sustained by diaphragm wall (Unit: m)

diaphragm walls are employed to support the foundation pit, then the deformation of surrounding rock converges to 3.5 mm. This indicates that both in-situ bored piles and diaphragm walls are effective in keeping the stability of foundation pit in the floor of the exit portal, but the deformation of rockmass dominated by bored piles is greater than that by diaphragm walls. In addition, the shear strain increment in the rockmass of the two cases is also obtained and illustrated in detail in Fig. 22 and Fig. 23 separately.

Comparison between Fig. 22 and Fig. 23 is performed and shows that the shear strain increment in rockmass around abutment foundation pit strutted by in-situ bored piles appears to be similar with the one in rockmass around foundation pit supported by diaphragm walls. It is also deduced from Fig. 22 and Fig. 23 that, whether the foundation pit is strutted by piles or by diaphragm walls, the maximum shear strain increment appears at the two toes of the tunnel sidewalls, but there is little difference in numerical value.

Consequently, it is easily deduced from the numerical simulation of excavating the rockmass in the abutment foundation pit that in-situ bored piles as well as diaphragm walls can be applied to maintain the stability of the foundation pit in the floor of the exit portal of Wang Deng tunnel. In order to analyze the deformation of the slope due to the excavation of the foundation pit for the bridge abutment, the limit equilibrium state of the slope is finally attained in the numerical simulation using strength reduction technique, and then the isogram of shear strain increment is also obtained and shown in Fig. 24 and Fig. 25 respectively.

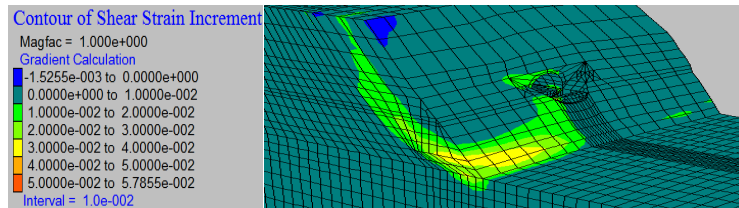


Fig. 24 Shear strain increment in slope with foundation pit sustained by piles (Unit: m)

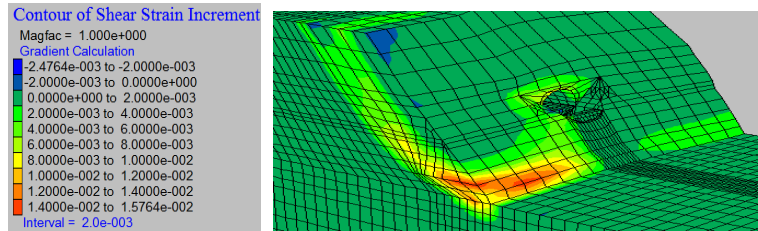


Fig. 25 Shear strain increment in slope with foundation pit sustained by diaphragm walls (Unit: m)

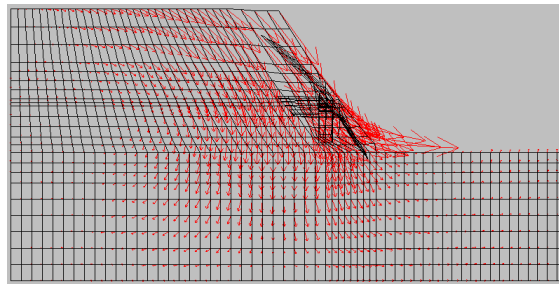


Fig. 26 Displacement vector in slope sustained by in-situ bored piles

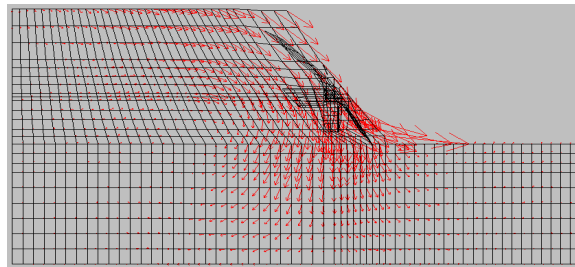


Fig. 27 Displacement vector in slope supported by diaphragm walls

Fig. 24 and Fig. 25 show the shear strain increment distributed in the slope as the slope reaches the limit equilibrium state; its maximum value appears at the toe. This again indicates that the slope may possibly collapse providing that the stability of its toe fails. It is also obtained that the excavation of rockmass in the foundation pit of bridge abutment does not obviously impact the stability of the whole slope, but the slope stability is dictated by the stress state of its toe. It is also derived that the value of shear strain increment distributed in the slope is different, its maximum in Fig. 24 reaches 5.79×10^{-2} , but the one in Fig. 25 is 1.58×10^{-2} , the former is approximately 3.7 times greater than the latter, this elucidates that the influence of excavating the rockmass in foundation pit on the deformation of slope is much less provided that the foundation pit is retained by diaphragm walls.

In addition, the nodal displacement vector in the two numerical models is obtained and illustrated in Fig. 26 and Fig. 27 respectively.

Fig. 26 shows the trend of rockmass displacement in the slope in which the bridge abutment foundation pit is to be excavated under the support of bored piles, and Fig. 27 shows the tendency of rockmass deformation in the slope in which the abutment foundation pit is to be excavated under the support of diaphragm walls.

It is inferred from Fig. 26 and Fig. 27 that the slope exists in the limit equilibrium state provided that the excavation of rockmass in the bridge abutment foundation pit is completed, meanwhile, the nodal displacement at the toe of the slope approaches the maximum value. This also indicates that slope failure may occur if its toe collapses at first. According to the numerical simulation, the safety factor of the slope which exists in the limit equilibrium state is different during the course of excavating rockmass in the foundation pit under the support of the two different retaining structures. When the foundation pit is sustained by in-situ bored piles, the obtained safety factor meets $F_s=1.42$. If the foundation pit is supported by diaphragm walls, then $F_s=1.53$. It's clearly seen that the excavation of foundation pit can diminish the safety factor of the whole slope, and the former is greater than the latter. This also denotes that diaphragm wall is much more efficient in keeping both the safety of foundation pit and the whole slope in comparison with in-situ bored piles. Additionally, in-situ bored piles are easier to be built in working site in comparison with diaphragm wall, meanwhile, the cost to build bored piles is much less than that to build diaphragm walls. Furthermore, it is easily deduced from formula $F_s=1.42$ that the slope still remains stable provided that bored piles are employed to sustain the foundation pit in the floor of the exit portal of Wang Deng tunnel according to $F_s=1.42>1.3$. Moreover, the crown settlement and sidewall convergence are all controlled within allowable value. As a result, In-situ bored piles can be still applied to sustain the abutment foundation pit in the exit portal of Wang Deng tunnel. The slope stability can be maintained during the tunneling of the exit portal on the high and steep slope reinforced by in-situ bored piles.

6. Conclusions

From the preceding numerical analysis of the stability of a high and steep slope due to the construction of an exit tunnel portal with bridge-tunnel combination, it is clear that the stability of high and abrupt slope is principally dictated not only by the strength of surrounding rock, the occurrence of rockmass, ground water, but also by the very typical structure of tunnel portal. After the numerical simulation of the tunneling procedure of the exit portal of Wang Deng tunnel on high and abrupt mountainous slope in Chengdu to Lanzhou express railway line, several useful conclusions can be drawn as follows.

(1) With respect to high and steep mountainous slope in express railway line, post tunnel portal is the preferred structure to fit high and steep slope in rugged areas.

(2) In-situ bored piles as well as diaphragm walls can be employed to enhance slope stability during tunnel construction and its long-term service. Though diaphragm wall is more superior to upholding the stability of high and steep slope in comparison with in-situ bored pile, the latter is in preference to the former in respect of the difficulty in the construction procedure, time limit as well as cost control. As a result, it is clear that bored pile can be used in the structural design and construction of the exit portal of Wang Deng tunnel.

(3) The high and abrupt slope on which the exit portal of Wang Deng tunnel is to be built remains safe and stable providing that the surrounding rock is reinforced with in-situ bored piles prior to excavation. The excavation of rockmass in the foundation pit sustained by in-situ bored piles for building bridge abutment in the floor of the exit portal of Wang Deng tunnel does not lower the entire stability of the high and steep slope.

(4) When building the exit portal and the bridge-tunnel combination on the high and steep slope, the first step is to reinforce the surrounding rock with bored piles so as to keep the stability of

rockmass, then to excavate the rockmass underneath the bridge abutment, finally to bore the tunnel exit portal using drill and blast method, simultaneously, the primary support is also required to be installed in as shorter time as possible.

Acknowledgments

The authors are grateful to the financial support provided by the National Natural Science Foundation of China (Grant No. 51378436) and the technical development program of the China Railway Corporation (No. 2010G018-C-1-3).

References

- Cala, M. and Flisiak, J. (2001), "Slope stability analysis with FLAC and limit equilibrium methods", *FLAC and Numerical Modelling in Geomechanics*, A. A. Balkema Publishers, Rotterdam.
- Carranza-Torres, C. (2009), "Analytical and numerical study of the mechanics of rockbolt reinforcement around tunnels in rock masses", *Rock Mech. Rock Eng.*, **42**(4), 175-228.
- Cheng, Y.M. and Yip, C.J. (2007), "Three-dimensional asymmetrical slope stability analysis extension of Bishop's, Janbu's, and Morgenstern-Price's Techniques", *J. Geotech. Geoenviron. Eng.*, ASCE, **133**(12), 1544-1555.
- Dawson, E.M., Roth, W.H. and Drescher, A. (1999), "Slope stability analysis by strength reduction", *Geotechnique*, **49**(6), 835-840.
- Duncan, J.M. (2000), "Factors of safety and reliability in geotechnical engineering", *J. Geotech. Geoenviron. Eng.*, ASCE, **126**(4), 307-316.
- GB50330 (2002), *Technical Code for Building Slope Engineering*, Compiled by the Ministry of Housing and Urban-Rural Development of the P.R.C. Beijing, China Architecture and Building Press. (in Chinese)
- Huang, C. and Tsai, C. (2000), "New method for 3D and asymmetric slope stability analysis", *J. Geotech. Geoenviron. Eng.*, ASCE, **126**(10), 917-927.
- Kocka, M.K. and Akgun, H. (2003), "Methodology for tunnel and portal support design in mixed limestone, schist and phyllite conditions: a case study in Turkey", *Int. J. Rock Mech. Min. Sci.*, **40**, 173-196.
- Kocka, M.K. and Akgun, H. (2005), *Tunnel and portal stability assessment in weak rock. Underground Space Use*, Taylor & Francis Group, London.
- Lee, I.K., White, W. and Ingles, O.G. (1983), *Geotechnical Engineering*, Pitman publishing Inc.
- Li, Y. and Li, T. (2012), "Analysis of nonlinear seismic response and stability for tunnel portal slope", *Appl. Mech. Mater.*, **160**, 263-267.
- Liu, S., Zhao, W., Zhang, Y., Gao, H. and Fu, F.. (2012), "Stability analysis of highway tunnel portal slope in Shiyan area", *Adv. Mater. Res.*, **368-373**, 2824-2827.
- TB10003 (2005), *Code for Design of Railway Tunnel*, Compiled by the 2nd Survey and Design Institute of China Railway, Beijing: China Railway Press. (in Chinese)
- Zhang, W., Jiao, Y. and Guo, X. (2008), "Slope stability analysis and prevention method of tunnel portal slope", *Rock Soil Mech.*, **29**, 311-314. (in Chinese)
- Zhang, M., Huang, R. and Ju, N. (2008), "Deformation mechanism and stability analysis of a high slope at portal of compressed tunnel at shallow depth", *J. Eng. Geology*, **16**(4), 482-488. (in Chinese)
- Zheng, Y. and Zhao, S. (2004), "Application of strength reduction FEM in soil and rock slope", *Chin. J. Rock Mech. Eng.*, **23**(19), 3381-3388. (in Chinese)
- Zhou, X., Jiang, B., Yang, R. and Ning, C. (2014), "Design of high speed railway tunnel and its construction method in abrupt slope with loose rockmass", *Appl. Mech. Mater.*, **580-583**, 1096-1099.
- Zhou, X., Wang, J. and Lin, B. (2014), "Study on calculation of rock pressure for ultra-shallow tunnel in

- poor surrounding rock and its tunneling procedure”, *J. Modern Tran.*, **22**(1), 1-11.
- Zhou, X., Wang, J., Hu, H. and Wang, X. (2013), “Structural design of highway tunnel in loose surrounding rock and its tunneling procedure”, *International Conference on Transportation*, 80-87.
- Zhou, X. (2014), “Structural design of mountain tunnels in the 3rd pipeline project of natural gas transmission from west to east China”, *Adv. Mater. Res.*, **1049-1050**, 217-220.
- Zhou, X., Jiang, B., Zhou, Y. and Yu, Y. (2014), “Design of rational concatenation between bridge and portal for mountain tunnel on high and steep slope”, *Adv. Mater. Res.*, **716-717**, 351-354.
- Zhou, X., Jiang, B., Zhou, Y. and Yu, Y. (2014), “Typical portal structure for single track high speed railway tunnel in rugged mountainous area with high and abrupt slope”, *Adv. Mater. Res.*, **716-717**, 342-346.
- Zhu, W., Li, S., Li, S., Chen, W. and Lee, C.F. (2003), “Systematic numerical simulation of rock tunnel stability considering different rock conditions and construction effects”, *Tunnel. Underg. Space Tech.*, **18**, 531-536.